AIChE

Prevention of Adhesion Bands by Ibuprofen-Loaded PLGA Nanofibers

Fatemeh Jamshidi-Adegani
Dept. of Molecular Medicine, School of Medicine, Qazvin University of Medical Science, Qazvin, Iran

Dept. of Molecular Biology and Genetic Engineering, Stem Cell Technology Research Center, Tehran, Iran

Ehsan Seyedjafari
Dept. of Biotechnology, College of Science, University of Tehran, Tehran, Iran

Nematollah Gheibi
Dept. of Physiology and Medical Physics, Qazvin University of Medical Sciences, Qazvin, Iran

Masoud Soleimani
Dept. of Molecular Biology and Genetic Engineering, Stem Cell Technology Research Center, Tehran, Iran

Dept. of Hematology, Faculty of Medical Science, Tarbiat Modares University, Tehran, Iran

Mehdi Sahmani
Dept. of Clinical Biochemistry and Genetics, Cellular and Molecular Research Center, Faculty of Medicine, Qazvin University of Medical Sciences, Qazvin, Iran

DOI 10.1002/btpr.2270
Published online August 3, 2016 in Wiley Online Library (wileyonlinelibrary.com)

In this study, prevention of the adhesion bands and inflammatory features has been investigated using poly (lactic-co-glycolic acid)-ibuprofen (PLGA-IB) nanofibrous meshes in a mice model. To find the optimized membrane for prevention of postoperative adhesion bands, we have compared PLGA-IB group with PLGA, IB, and control groups in a mice adhesion model. Two scoring adhesion systems were used to represent the outcome. According to the results obtained in this study, the PLGA-IB nanofiber membrane showed a greater reduction in adhesion band than other groups. In conclusion, among FDA-approved polymers and drugs, PLGA-IB meshes could be applicable as a potential candidate for prevention of post-operative abdominal inflammation and adhesion bands formation. © 2016 American Institute of Chemical Engineers *Biotechnol. Prog.*, 32:990–997, 2016
Keywords: intraperitoneal adhesion, poly(lactic-co-glycolic acid), ibuprofen

Introduction

Wound healing is a complex process in which a series of cellular and humoral components interact to re-epithelialize a wound defect.[1] Peritoneal adhesions are a worldwide problem and may occur following any type of abdominal or pelvic surgery. They are fibrous bands that form between tissues and organs. These bands are the consequence of inflammatory reactions after damage to the peritoneum and have been well recognized as an important part of the wound healing process.[2] Invasive surgery is typically accompanied by a number of clinical problems, induced or exacerbated by adhesion bands, including female infertility, bowel obstruction, and difficult reoperative procedures. Adhesion bands have often been reported in clinical patients with foreign body reaction/infection, trauma, ischemia, and hemorrhage.[2–6]

The hope now is to identify agents that would efficiently reduce the formation of adhesion in various surgical procedures without inducing side effects. In moving toward this goal, different strategies such as various surgical techniques, surgical adjuvants for example fibrinolytic agents, anticoagulants, anti-inflammatory agents, antibiotics, different barriers and mechanical separation have been tested to prevent or at least diminish the high incidence of adhesions in patients.[4] Among these strategies, it seems physical barriers are one of the most accepted methods for prevention of adhesion formation.[7]

An antiadhesive barrier not only should have appropriate mechanical properties to facilitate handling and manipulation but also needs to possess suitable biomaterial surface hydrophilicity from the point of view of surface chemistry. A reduced amount of cell attachment is often seen on surfaces with a high hydrophilic nature.[8,9]

Previous finding have provided evidence that synthetic polymeric materials are preferable to natural agents in this context, mainly due to their ease of handling and lower level of immunogenicity. The principal objective of using synthetic barriers is to prevent mechanical contact between tissues around the damaged site to reduce these bands during the important period of peritoneal repair and healing. By reducing the formation of a fibrin matrix between serosal

Correspondence concerning this article should be addressed to Mehdi Sahmani at m.sahmani@gmail.com or Masoud Soleimani at soleim_m@modares.ac.ir

surfaces and implanted materials, synthetic barriers act to prevent the formation of adhesion bands.[10]

Electrospun fibers have found applications in tissue engineering, biomolecule immobilization, nutraceutical delivery, biosensing, bioremediation, and in the development of antimicrobial mats and etc.[11–13]

Recently, electrospun nanofibrous membranes have emerged as hopeful antiadhesion barriers. Electrospun membranes have attracted the interest of research for some time because of their bulk semi conductivity and, in some cases, one-dimensional ohmic conductivity. Electrospinning is a process by which fabricated polymeric membranes can be produced with nanofibrous structure in a simple, versatile, and economical manner. The application of electrospun nanofibrous membranes in preventing adhesion bands was described for the first time by Zong et al.[14] Thereafter, several applications of this membrane have been reported in the field of tissue engineering and regenerative medicine. For instance, the polycaprolactone (PCL) electrospun membranes have been effectively used in reduction of postoperative adhesions in a study conducted by Chen et al.[15,16] In view of the above findings, in the current study investigated the antiadhesive and anti-inflammatory effects of electrospun nanofibrous membranes made of PCL, poly-L-lactide (PLLA), poly(lactic-*co*-glycolic acid) (PLGA), and polyethersulfune (PES) in comparison with the oxidized-regenerated cellulose (Interceed) that has been approved by FDA for clinical use. Our results revealed that compared with other membranes, PCL, PLGA, and Interceed membranes showed a greater ability to reduce adhesions. Moreover, PLGA nanofibrous membranes showed the lowest level of both cell attachment in vitro and inflammation in adhesive tissues.[9]

Given that inflammation is a primitive protective response following surgical operation, determining ways of decreasing inflammation is of great interest. Ibuprofen (IB) is introduced as a nonsteroidal anti-inflammatory drug and is used to reduce fever and treat pain or inflammation caused by many conditions.[7,10] In this regard, Hu et al.[7] showed that PLLA containing IB improves anti-inflammatory activity in the prevention of peritendinous adhesions. Due to the ability of PLGA in reduction of peritoneal adhesion bands and IB role as an anti-inflammatory drug, in this study, we hypothesized PLGA nanofibrous scaffolds containing IB might prevent intra-abdominal adhesion formation, along with decreasing inflammation at the site of injury. Actually, we decided to evaluate the anti-inflammatory effect of IB on adhesion formation by incorporating PLGA nanofibers in an abdominal adhesion mice model.

In the present study, IB-incorporated PLGA was fabricated using the electrospinning method, and after characterization, their antiadhesion potential was compared to PLGA, IB and control groups in a mice model.

Materials and Methods

Electrospun nanofiber fabrication

A PLGA (5 wt %) solution was prepared by dissolving PLGA in chloroform/DMF (3/1 v/v) under constant stirring for 2 h at room temperature. For preparation of the PLGA solution containing IB, IB with a weight ratio of 10% w/w referred to the PLGA were dissolved in 2 mL chloroform and then added to a 4 wt % PLGA solution under constant stirring for 4 h to obtain a uniform solution. IB-loaded nanofiber meshes were obtained by one-step two-nozzle electrospinning of PLGA/IB and PLGA solutions.

The electrospinning experimental setup was a Nano Model (Tehran, Iran) with two nozzles. During electrospinning, positive 20 and 18 kV charges were applied at the tip of the syringe needle for PLGA-IB and PLGA, respectively. The PLGA and PLGA-IB mass flow rates were maintained at 0.5 and 0.4 mL/h, and the operating distances were selected at 20 and 15 cm, respectively. A rotary aluminum foil collector with 300 rpm was used. Application of a voltage between the needle and the collector forced the solution droplets to leave the needle and spread on a cylinder in the form of ultrafine fibers.[17,18]

Electrospun nanofiber characterization

Scanning Electron Microscopy. Fabricated PLGA and PLGA-IB scaffolds were morphologically characterized by using scanning electron microscopy (SEM, Philips XL30, Netherlands).The samples were gold coated using a sputter coater and then scanned by an SEM. The mean fiber diameter was obtained by manual microstructure distance measurement software, Nahamin Pardazan Asia.

Attenuated Total Reflection–Fourier Transform Infrared Spectroscopy. Attenuated total reflection–Fourier transform infrared (ATR-FTIR) analysis was used to evaluate and confirm the IB presence in composite scaffolds (PLGA-IB). The spectra were recorded using an Equinox 55 spectrometer (Bruker Optics, Germany) equipped with a DTGS (Deuterated TriGlycine Sulfate) detector and a diamond ATR crystal.

Mechanical properties. Mechanical behavior of nanofiber samples were characterized through tensile test on an Instron universal testing machine (Model STM-20, SANTAM, Iran), with sample sizes of 30×10 mm^2 and a loading velocity of 50 mm/min. The results are based on four samples punched from a single electrospun sheet. The machine recording data were used to plot the tensile stress–strain curves.

Ibuprofen release behavior. PLGA-IB nanofibrous meshes (weight 25 g) were immersed in 10 mL PBS then incubated at 37°C for 7 days with mild shaking (100 rpm). At specified time intervals, 1 mL of release medium was collected and replaced with 1 mL of fresh PBS. The amount of IB in the released samples was determined by UV–vis spectroscopy at 264 nm. A standard calibration curve of IB in the concentration range of 0–0.05 mg/mL (absorbance at 264 nm) was used to determine the IB concentration of released samples. Triplicate specimens were investigated. The accumulated IB released percent was calculated based on the initial weight of IB incorporated in the electrospun membranes. The results are presented in terms of cumulative release, which was calculated according to the cumulative amount of release equation:

$$\mathrm{Ib}_j = C_j V + \sum C_{j-1} V_s \tag{1}$$

The total mass of released IB, Ib_j at Time j was calculated from the mentioned equation, where C_j is the concentration of released IB in the solution at Time j, V is the total volume of release solution, and V_s is the sample volume.

Table 1. Adhesion and Inflammation Classifications

Grade	Züuhlke et al.	Duran et al.	Inflammation
0	No adhesion	No adhesion	Nil
1	Filmy adhesions: gentle, blunt dissection required to free adhesions	25% of area	Giant cells, occasional scattered lymphocytes and plasma cells
2	Mild adhesions: aggressive blunt dissection required to free adhesions	25–50% of area	Giant cells with increased numbers of admixed lymphocytes, plasma cells, eosinophils, neutrophils
3	Moderate adhesions: sharp dissection required to free adhesions	50–100% of area	Many admixed inflammatory cells, microabscesses present
4	Severe adhesions: not dissectible without damaging organs	–	–

Surgical technique

In the present study, the surgical procedures for this investigation were performed in accordance with the Stem Cell Technology Research Center (Tehran, Iran) guidelines. Totally, 28 male NMRI mice (from Razi Institute, Karaj, Iran) with weight ranging from 25 to 30 g were divided by chance into four groups of seven as follow: Group 1, surgical abrasion without any treatment as control ($n = 7$); Group 2, surgical abrasion plus PLGA nanofibers ($n = 7$); Group 3, surgical abrasion plus IB ($n = 7$); Group 4, surgical abrasion plus composite scaffolds (PLGA-IB) ($n = 7$).

The animals were kept in cages ($n = 7$ in each) at a temperature of a temperature of 21 ± 2°C and 12/12 h light/dark conditions. The surgical treatment was performed under general anesthesia induced by ether and ketamine (3 mg/kg) in combination.

The adhesion induction model described by Hemadeh et al.[19] was used, which resulted in a 100% incidence of adhesions in our control mice. Briefly, following anesthetic induction, animals were placed in a supine position for shaving and sterilization with alcohol and povidine iodine solutions. A vertical midline incision of 2 cm was made in the skin and the abdomen was opened. The exposed cecum was then gently abraded using dry gauze pads at all surfaces until it lost its shine, and hemorrhagic points became visible without perforation. After that, the cecum was returned to its anatomic position in the abdominal cavity. Before closing the abdomen, 1.5×1.5 cm piece of each type of membrane were sutured between the abdominal wall and peritoneum. In the IB group, 1-mL IB solution 2 mg/mL was injected to the abdomen. The abdominal wall was sutured in two layers. After 1 week, mice were euthanized and their abdominal cavities reopened evaluated by two other surgeons. The post-surgical adhesion band was assessed based on previously explained scales, based on two scales explained by Zühlke et al. and Duran et al. as shown in Table 1.[20,21]

Microscopic examination

After sacrificing the animals, microscopic examination of the morphology of the surgical location was performed to look for signs of inflammation, infection and complications, and images were captured.

Histologic evaluation

The nanofibers and the peritoneal tissues around them were extracted following evaluation from the other tissues, and then fixed in 10% formalin and immersed in paraffin. Several paraffin sections were made by microtome and stained by hematoxylin–eosin (HE). A semi quantitative scoring system was used to evaluate the degree of inflammation, as indicated in Table 1.[22]

Biochemistry analysis. The mean cytokines such as interleukin 1 (IL-1), interleukin 6 (IL-6) and tumor necrosis factor-α (TNF-α) levels were determined by an ELISA method at 0, 3, and 7 days after surgery. Peritoneal fluid samples were collected in the ependorf tubes with 5% EDTA and were centrifuged in 4°C for 5 min in 3,000 rpm. The supernatant was collected for ELISA assay using the appropriate kits (Mouse IL-6, IL-1, TNF-α Platinum ELISA kit/EBioscience Company). Each sample was distributed in triplicate. Microsoft Excel was used for drawing standard curves and ELISA results.

Statistical analysis

All variables were expressed as mean ± SD and ranks. Differences between the adhesion and inflammation scores were evaluated by Kruskal–Wallis variance analysis and when significant ($P < 0.05$), the difference between specific mean ranks was determined using the multiple comparison procedure based on ranks.

Results

Scaffold characterization

Fabricated PLGA nanofibrous scaffolds showed a porous structure, beads-free, uniform and smooth morphology with an average diameter of 300 ± 500 nm (Figure 1a,b with low magnification). It was also obvious that the morphology and diameter of PLGA nanofibers was not significantly affected by incorporating IB (Figure 1c,d).

PLGA mats showed a tensile strength of 2.72 ± 0.94 MPa and elongation at break of $49.80 \pm 5.84\%$. These properties were improved significantly after IB incorporating (strength of 11.73 ± 4.43 MPa and elongation at break of $76.63 \pm 21.53\%$) which is due to the fact that crystalline IB added to amorphous PLGA, increase mechanical properties of IB-loaded PLGA meshes compared to the PLGA ones. The release profile of IB from IB-loaded PLGA nanofibrous scaffolds is shown in Figure 2. The release mechanism is combined of degradation and diffusion. Almost 30% of loaded IB released within about 8 h without any initial burst release and then 50% of total IB has been released during only 4 h; same release pattern has been reported by Pang et al.[23] It is predicted that remained IB will release in the prolonged time.

Fourier Transform Infrared. FTIR spectroscopy is widely employed for analyzing chemical components and identifying characteristic groups. As shown in Figure 3, in the FTIR spectrum of IB, the major peak at 1,750 cm^{-1} was attributed to the C = O stretching vibration and the major

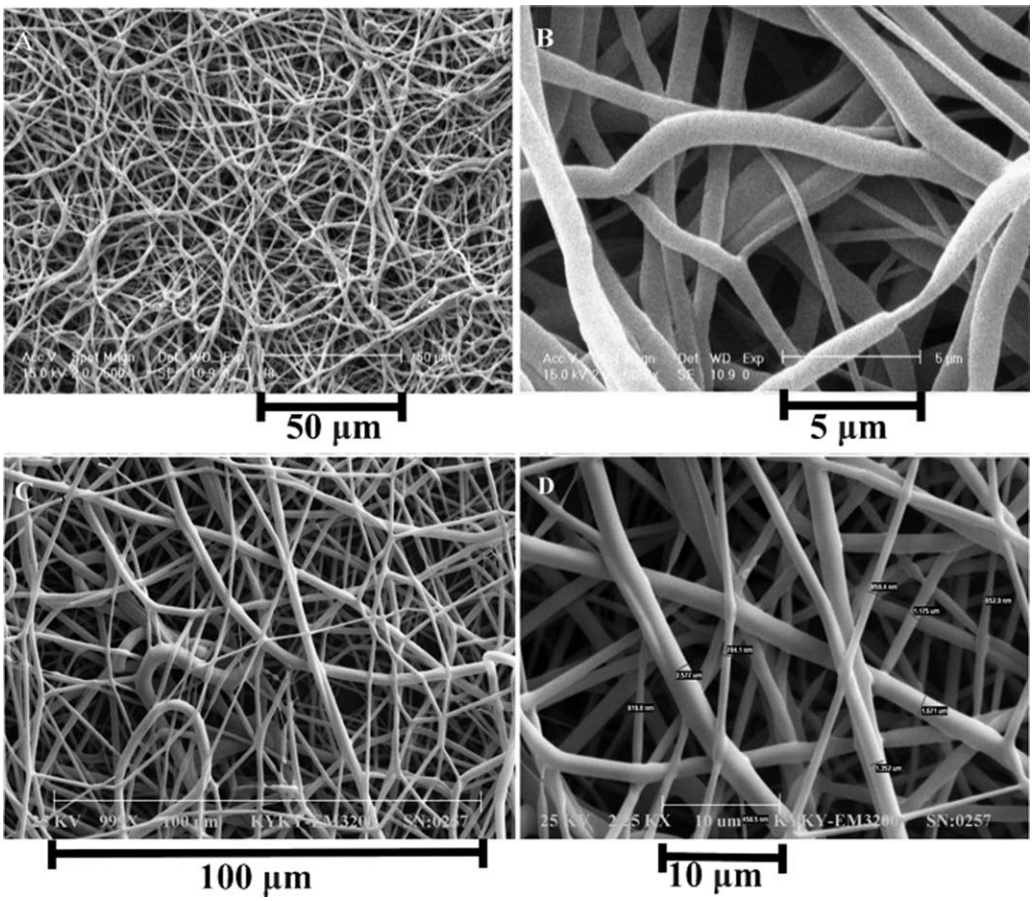

Figure 1. SEM photograph of PLGA (A, B) and PLGA-IB (C, D) nanofibrous scaffolds in high and low magnification.

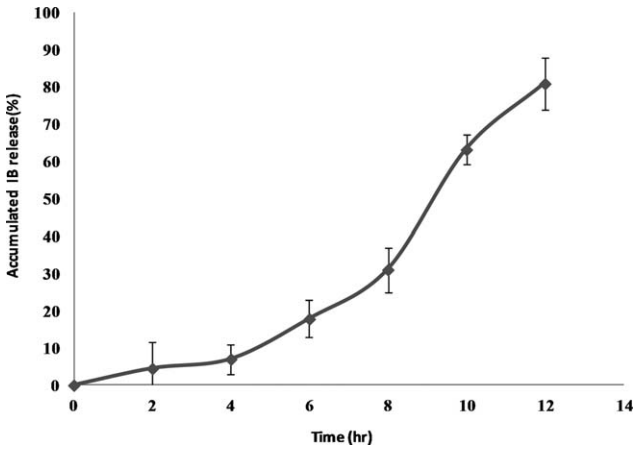

Figure 2. Release profile of IB from PLGA-IB nanofibrous scaffold ($n = 3$).

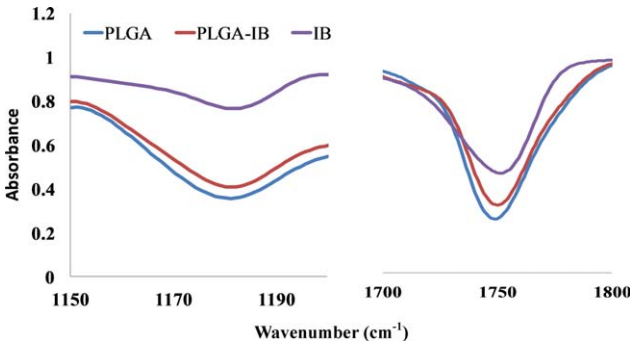

Figure 3. FTIR spectra in the regions 1,150 to 1,200 and 1,700 to 1,800 $cm^{-1}$of IB, PLGA, and PLGA/IB.

band from 1,150 to 1,200 cm^{-1} was assigned to the characteristic vibrations of C–O stretch modes of the alcohols. These characteristic peaks of IB can also be observed in the FTIR spectrum of PLGA and PLGA-IB scaffolds. The spectrum of the PLGA-IB is more similar to that of the IB, which confirms that IB was incorporated into the PLGA scaffold.

The Grade of Adhesion Bands. No mortalities were observed during or end of the study, abdominal adhesion score was evaluated according to the Zühlke and Duran et al. scaling that is shown in Figure 4. Significantly highest decrease of adhesion score observed in animals were implanted with PLGA-IB ($P < 0.01$), although animals treated with PLGA also exhibited a decrease of adhesion score in comparison to untreated control groups ($P < 0.05$).In addition, the adhesion scores of animals treated with IB alone did not significantly change in comparison to control groups. Images that illustrate the grades of abdominal adhesion are presented in Figures 5 and 6. Histological analysis was performed to further explore the role of PLGA-IB in the decrease of abdominal adhesion after surgery. The inflammation score of control group was dominant at the serosal surface of the cecum. As showed in Figure 7, there were inflammatory cells such as neutrophils, giant cells, plasma

cells, and lymphocytes around the peritoneal surface. Statistically significant differences were observed between PLGA-IB and PLGA groups with IB and control groups. Compared with all groups, a significant decrease of inflammation scores of mice following administration of PLGA-IB membrane was revealed ($P < 0.05$). The inflammation scores in all groups are shown in Figure 8.

Cytokine Assay. To determine the nature of the immune responses we measured the amount of IL-1, IL-6, and TNF-α produced in the supernatant at 0 and 3, 7 days after surgery. As shown in Figures (9, 10), and 11, there are an increase in IL-1, IL-6, and TNF-α after surgery compared to Day 0 but the amount of IL-6 and TNF-α decrease significantly in PLGA and PLGA-IB groups, the production level of IL-6 and TNF-α was significantly lower in PLGA-IB group than the production level of these cytokines in other groups at 7 days after surgery.

According to Figure 9, IL-1 production was decreased in all groups of mice after 7 days; however, a small decrease in IL-1 occurred at 7 days postsurgery in PLGA-IB group compared to other groups.

In conclusion, production of TNF-α and IL-6 were decreased significantly in PLGA + IB group compared with another groups.

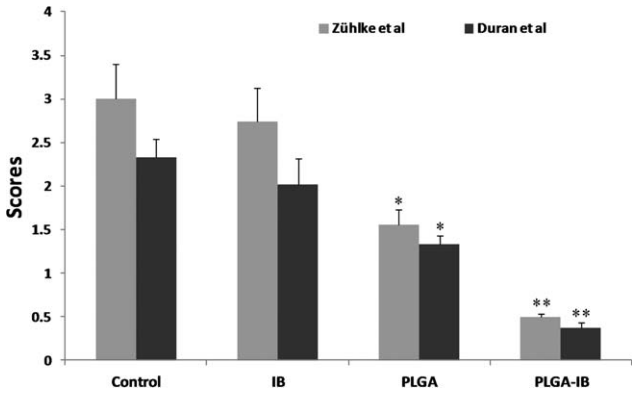

Figure 4. Adhesion scores of each group using two scaling systems; the results are shown as mean ± SD. The significant difference ($P < 0.05$) has been shown between the PLGA + IB group with the control group, there is not a significant difference between IB group with control group.

Discussion

Peritoneal adhesion commonly occurs after abdominal surgery. It is necessary to mention that an adhesion is a band between the cicatrix of surgery tissue and the peritoneal membrane or gut which causes to stick together.[6,15] This untoward outcome is a challenge for surgeons and patients; moreover, this problem also increases the cost of health care after surgery. Recently, several biomaterials have been introduced as a physical barrier to solve or at least reduce this problem. For instance, Bölgen et al. incorporated an antibiotic in PCL and investigated its effect on rat abdominal wounds after surgery in comparison with those of PCL and control groups.[24] Their macroscopically and histological observations demonstrated that physical barriers could reduce the value and hardness of postsurgery adhesion bands. They also reported that there is a significant diminishing of adhesion bands was detected when animals treat with antibiotic-loaded PCL.[24] Some researchers reported that implantation of common biodegradable polymers such as poly(glycolic acid) and poly(lactic acid) without antibiotic at the site of surgery will cause severe inflammation due to the acidic nature of the PCL.[25,26] As IB suppresses inflammation, we decided to load IB into PLGA and fabricate electrospun nanofibers using this mixture.

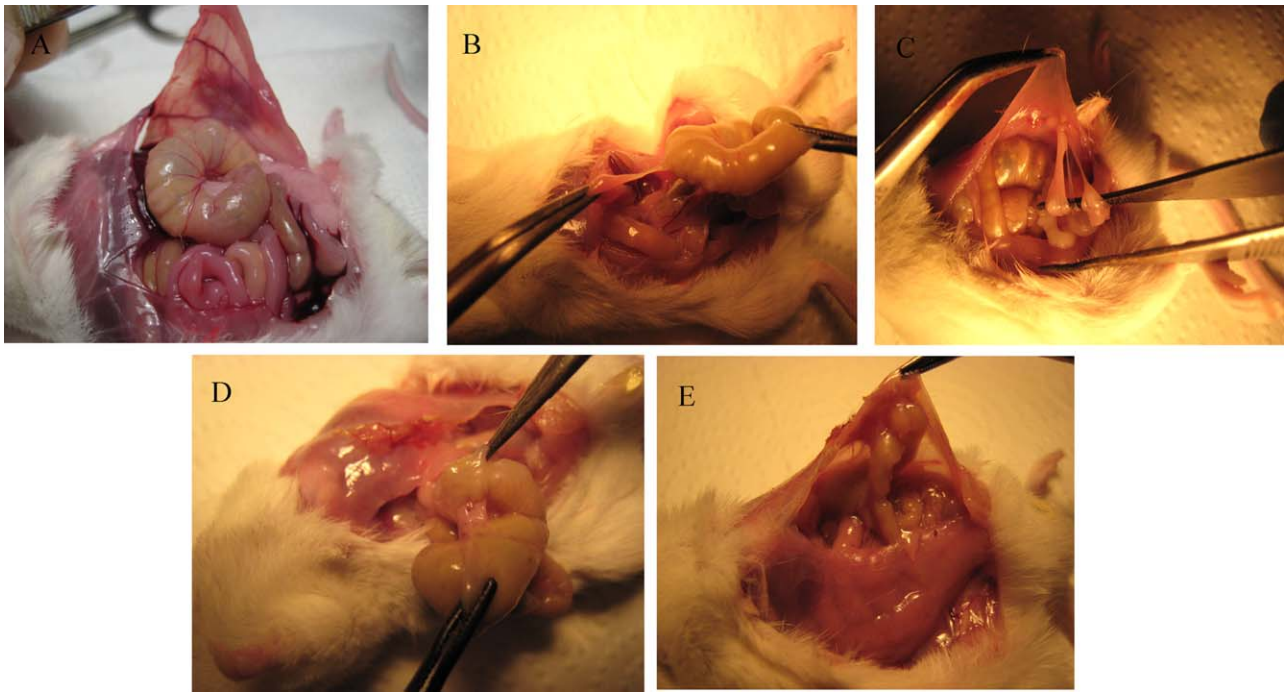

Figure 5. Images show the intraperitoneal adhesion formation in mice according to Zühlke et al. (A) Grade 1, filmy adhesions: gentle, blunt dissection required to free adhesions. (B) Grade 2, mild adhesions: aggressive blunt dissection required to free adhesions. (C) Grade 3, moderate adhesions: sharp dissection required to free adhesions. (D and E) Grade 4, severe adhesions: not dissectible without damaging organs.

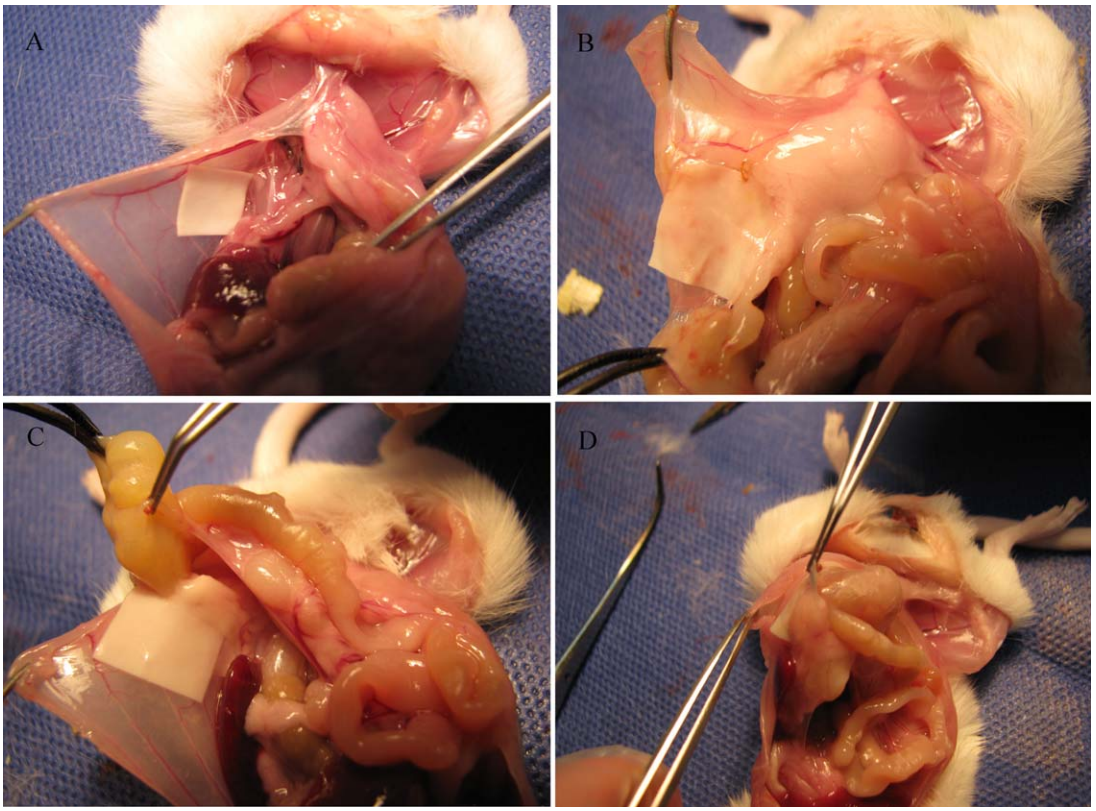

Figure 6. Illustrations show the adhesion bands between peritoneum and abdominal wall in mice according to Duran et al. (A) Grade 0, no adhesion band. (B) Grade 1, 25% of area of membrane. (C) Grade 2, 25–50% of area of membrane. (D) Grade 3, 50–100% of area of membrane.

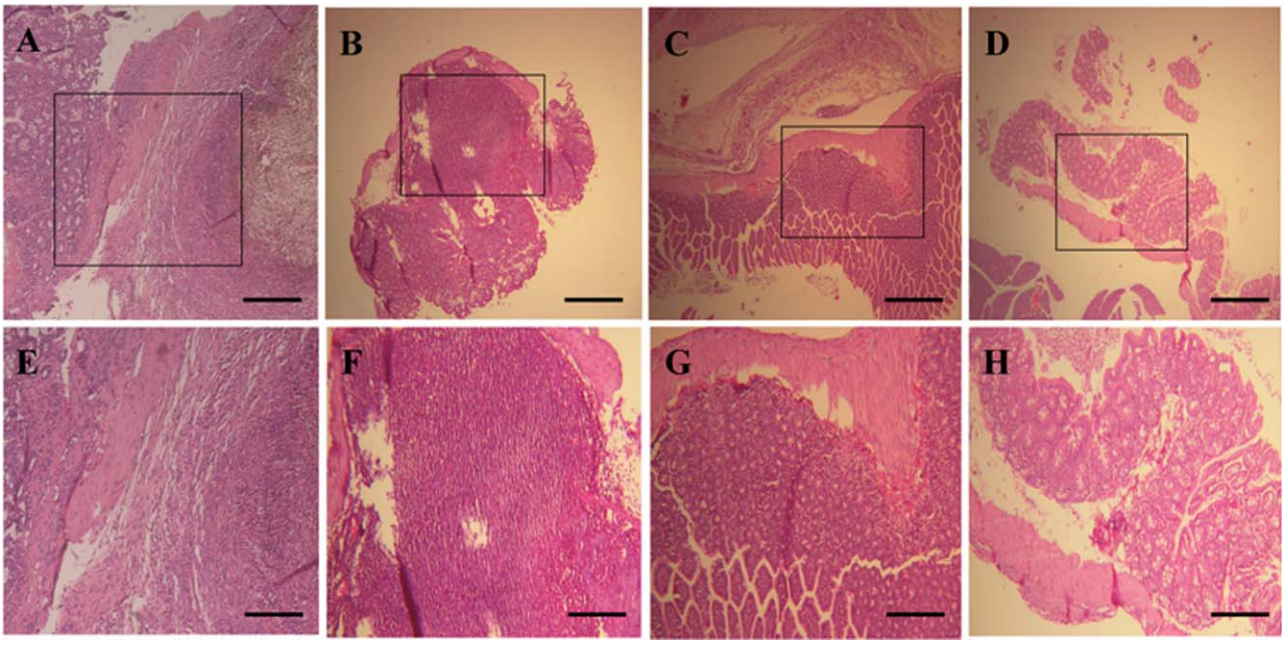

Figure 7. Representative images of histological observations in two magnifications: for the control group (A) and (E); for the IB group (B) and (F); for the PLGA group (C) and (G); for the PLGA + IB group (D) and (H).

Antiadhesive band formation sutures of this construct were investigated in a mouse abdominal adhesion model and were compared with PLGA, IB, and control groups. SEM images of PLGA-IB nanofibers confirmed that the nanoscale and morphology were not significantly different before and after IB incorporation. Electrospinning has been used to load several drugs in nanofibrous scaffolds as drug carriers, these nanofibers playing a modulator role in drug release. Our drug release analysis demonstrated a growing and sustained trend of IB diffusion from the PLGA nanofibers into the medium during the 12-h assay.

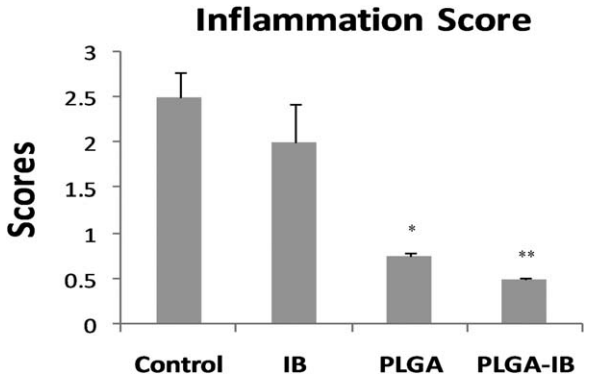

Figure 8. Inflammation scores of each group; the data are shown as mean ±SD. The significant difference ($P < 0.05$) has been shown between the groups with (*) and all other groups (**) and the control group.

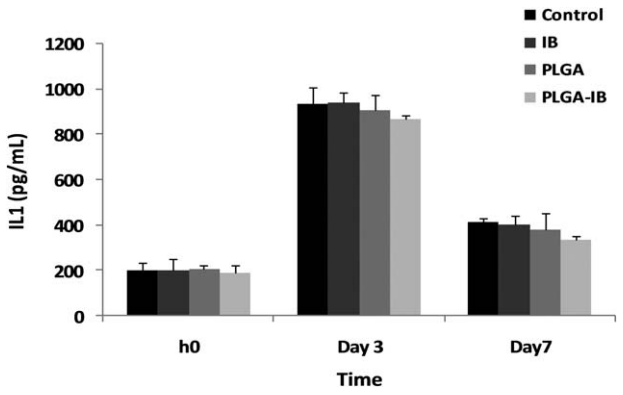

Figure 9. The means cytokine (1L-1) level at Day 0 and at Day 3, 7 days after surgery. The results represent that there is not a significant difference between groups.

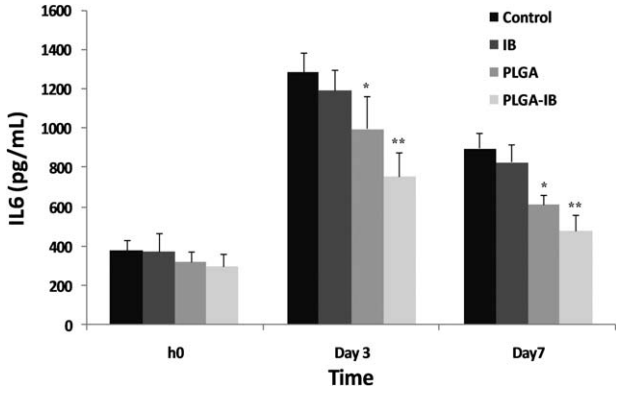

Figure 10. The means cytokine (1L-6) level at Day 0 and at Day 3, 7 days after surgery. The results represent that at Day 3 and Day 7, there is a significant difference between PLGA + IB group with another groups.

The results of the animal adhesion model demonstrated that both electrospun nanofibrous PLGA and IB-PLGA mats had antiadhesive and anti-inflammatory properties and also that these properties significantly improved after IB incorporation in PLGA. Anti-inflammatory effects of this construct could be related to the efficient release of IB from PLGA nanofibers on the one hand; on the other hand, these properties may result from the synergistic effects of PLGA as a

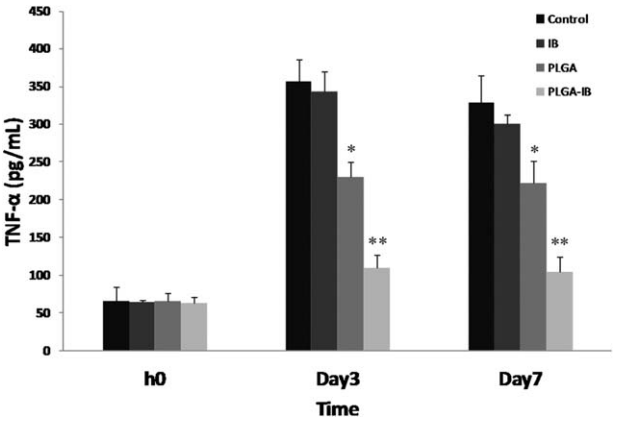

Figure 11. The means cytokine (TNF_α) level at Day 0 and at Day 3 7 days after surgery. The results represent that, at Day 3 and Day 7, there is a significant difference between PLGA + IB group with another groups.

physical barrier and IB. These results are consistent with our previously reported study where antiadhesive and anti-inflammatory effects of PLLA, PCL, PES, and PLGA electrospun nanofibers were evaluated in a mouse model compared with the effects of oxidize-regenerated cellulose (Interceed) as a positive control. The results showed that PLGA had the lowest adhesion and inflammation scores among mice treated with PES, PLGA, PLLA, PCL, and Interceed and also among untreated mice.[9] In another study, antiadhesive and anti-inflammatory results of animals treated with PLGA were inconsistent with our study; there was no significant difference between the PLGA group and the untreated group due to high hydrophobicity and shrinkage. In our animal model, these properties were diminished by suture mats according to the procedure reported by Dinarvand et al., and for hydrophobicity conformation water contact angle was used, with the results demonstrating that contact angle of PLGA (112°C) was not altered after incorporation with IB.[9]

To confirm lower inflammation as a result of the PLGA-IB procedure, cytokines responsible for inflammation were evaluated using ELISA. The rates of IL-1, IL-6, and TNF-α in peritoneal fluid were found to be significantly decreased in animals treated with PLGA-IB in comparison to other groups. A mouse adhesion model was introduced for short-time assay, and this model in rats was appropriate for long-time assay. Inflammation is a phenomenon that occurs during the primary steps in formation of the adhesion band. For this reason, a week was selected as a time period for our study.

Conclusion

In this study, we have investigated the effect of PLGA-IB mats in prevention of adhesion band that form after surgery. Indeed, our results demonstrated that IB incorporated PLGA mats have shown enhanced antiadhesive and anti-inflammatory potentials in comparison to animals treated with PLGA and untreated animals during the period of study. This construct could be introduced as potentially candidate for physical barrier usage to prevention or diminish abdominal postsurgery inflammation and adhesion band formation.

Acknowledgment

The authors gratefully acknowledge the support of the Stem Cell Technology Research Centre (Tehran, Iran).

Literature Cited

1. Hwang K, Bianchi E, Sigman M, Lamb D, Boekelheide K. Special research presentation: defining the role of ghrelin in wound healing and the inflammatory response in the post-operative setting. *Fertil Steril* 2014;102:e2.
2. Greene AK, Alwayn IPJ, Nose V, Flynn E, Sampson D, Zurakowski D, Folkman J, Puder M. Prevention of intra-abdominal adhesions using the antiangiogenic COX-2 inhibitor celecoxib. *Ann Surg* 2005;242:140.
3. Guvenal T, Cetin A, Ozdemir H, Yanar O, Kaya T. Prevention of postoperative adhesion formation in rat uterine horn model by nimesulide: a selective COX-2 inhibitor. *Hum Reprod* 2001; 16:1732–1735.
4. Kamel RM. Prevention of postoperative peritoneal adhesions. *Eur J Obstet Gynecol Reprod Biol* 2010;150:111–118.
5. Lalountas M, Ballas K, Michalakis A, Psarras K, Asteriou C, Giakoustidis D, et al. Postoperative adhesion prevention using a statin-containing cellulose film in an experimental model. *Br J Surg* 2012;99:423–429.
6. Dinarvand P, Rezaie AR. Intraperitoneal administration of activated protein C prevents post-surgical adhesion band formation. *Blood* 2013;122:3581.
7. Hu C, Liu S, Zhang Y, Li B, Yang H, Fan C, et al. Long-term drug release from electrospun fibers for in vivo inflammation prevention in the prevention of peritendinous adhesions. *Acta Biomater* 2013;9:7381–7388.
8. Goldberg EP, Yaacobi Y. Method and composition for preventing surgical adhesions. *Google Patents* 1997;
9. Dinarvand P, Hashemi SM, Seyedjafari E, Shabani I, Mohammadi-Sangcheshmeh A, Farhadian S, et al. Function of poly (lactic-co-glycolic acid) nanofiber in reduction of adhesion bands. *J Surg Res* 2012;172:e1–e9.
10. Yeo Y, Kohane DS. Polymers in the prevention of peritoneal adhesions. *Eur J Pharm Biopharm* 2008;68:57–66.
11. Grodecki J, Short AR, Winter JO, Rao SS, Otero JJ, Lannutti JJ, et al. Glioma-astrocyte interactions on white matter tract-mimetic aligned electrospun nanofibers. *Biotechnol Prog* 2015; 31:1406–1415.
12. Konwarh R, Karak N, Misra M. Electrospun cellulose acetate nanofibers: the present status and gamut of biotechnological applications. *Biotechnol Adv* 2013;31:421–437.
13. Xu W, Yang W, Yang Y. Electrospun starch acetate nanofibers: development, properties, and potential application in drug delivery. *Biotechnol Prog* 2009;25:1788–1795.
14. Zong X, Li S, Chen E, Garlick B, Kim K-s, Fang D, et al. Prevention of postsurgery-induced abdominal adhesions by electrospun bioabsorbable nanofibrous poly(lactide-co-glycolide)-based membranes. *Ann Surg* 2004;240:910.
15. Chen S-H, Chen C-H, Fong YT, Chen J-P. Prevention of peritendinous adhesions with electrospun chitosan-grafted polycaprolactone nanofibrous membranes. *Acta Biomater* 2014;10:4971–4982.
16. Chen S-H, Chen C-H, Shalumon K, Chen J-P. Preparation and characterization of antiadhesion barrier film from hyaluronic acid-grafted electrospun poly (caprolactone) nanofibrous membranes for prevention of flexor tendon postoperative peritendinous adhesion. *Int J Nanomed* 2014;9:4079.
17. Seyedjafari E, Soleimani M, Ghaemi N, Shabani I. Nanohydroxyapatite-coated electrospun poly (l-lactide) nanofibers enhance osteogenic differentiation of stem cells and induce ectopic bone formation. *Biomacromolecules* 2010;11:3118–3125.
18. Hashemi SM, Soudi S, Shabani I, Naderi M, Soleimani M. The promotion of stemness and pluripotency following feeder-free culture of embryonic stem cells on collagen-grafted 3-dimensional nanofibrous scaffold. *Biomaterials* 2011;32:7363–7374.
19. Hemadeh O, Chilukuri S, Bonet V, Hussein S, Chaudry IH. Prevention of peritoneal adhesions by administration of sodium carboxymethyl cellulose and oral vitamin E. *Surgery* 1993;114: 907–910.
20. Lorenz E, Zühlke H, Lange R, Savvas V. Pathophysiology and Classification of Adhesions. Peritoneal Adhesions. Springer: Berlin, Heidelberg. 1997:29–34.
21. Duran B, Ak D, Cetin A, Guvenal T, Cetin M, Imir AG. Reduction of postoperative adhesions by N,O-carboxymethylchitosan and spermine NONOate in rats. *Exp Anim* 2003;52:267–272.
22. Hooker GD, Taylor BM, Driman DK. Prevention of adhesion formation with use of sodium hyaluronate–based bioresorbable membrane in a rat model of ventral hernia repair with polypropylene mesh—A randomized, controlled study. *Surgery* 1999; 125:211–216.
23. Pang J, Luan Y, Li F, Cai X, Du J, Li Z. Ibuprofen-loaded poly (lactic-co-glycolic acid) films for controlled drug release. *Int J Nanomed* 2011;6:659–665.
24. Bölgen N, Vargel I, Korkusuz P, Menceloğlu YZ, Pişkin E. In vivo performance of antibiotic embedded electrospun PCL membranes for prevention of abdominal adhesions. *J Biomed Mater Res B: Appl Biomater* 2007;81:530–543.
25. Heublein B, Rohde R, Kaese V, Niemeyer M, Hartung W, Haverich A. Biocorrosion of magnesium alloys: a new principle in cardiovascular implant technology? *Heart* 2003;89:651–656.
26. Anderson JM, Shive MS. Biodegradation and biocompatibility of PLA and PLGA microspheres. *Adv Drug Delivery Rev* 2012; 64:72–82.

Manuscript received Sep. 1, 2015, and revision received Mar. 31, 2016.